

# Preparation and oxygen sensing properties of Ti<sub>3</sub>O<sub>5</sub> submicron rods

Xiaoyan Zhang<sup>1</sup>, Wanying Liu<sup>1</sup>, Hua Yu<sup>1</sup>, Xiaoxi Zhong<sup>2</sup>, Lijun Wang<sup>1</sup>, Ambrish Singh<sup>1</sup>, Yuanhua Lin<sup>1,3</sup> ✉

<sup>1</sup>School of Materials Science and Engineering, Southwest Petroleum University, Chengdu, Sichuan 610500, People's Republic of China

<sup>2</sup>Sichuan Province Key Laboratory of Information Materials and Devices Application, Chengdu University of Information Technology, Chengdu 610225, Sichuan, People's Republic of China

<sup>3</sup>State Key Laboratory of Oil and Gas Reservoir Geology and Exploitation, Southwest Petroleum University, Chengdu, Sichuan 610500, People's Republic of China

✉ E-mail: yhlin28@163.com

Published in Micro & Nano Letters; Received on 22nd June 2016; Revised on 27th July 2016; Accepted on 24th August 2016

Ti<sub>3</sub>O<sub>5</sub> submicron rods, typically 0.5–2 µm in length and 100–300 nm in diameter, have been successfully synthesised via a facile approach combined hydrothermal and carbothermal reduction route. H<sub>2</sub>Ti<sub>3</sub>O<sub>7</sub> nanofibres blended with nano-sized carbon black were first prepared by the direct hydrothermal processing, and then Ti<sub>3</sub>O<sub>5</sub> submicron rods could be obtained by sintering the prepared nanofibres at 1250°C for 3 h. The microstructure and formation of phases in the reduction process were investigated, respectively. In addition, the oxygen sensing properties of the synthesised materials were preliminarily investigated by gas-sensing measurement. The results indicated that the electrical conductivity of the Ti<sub>3</sub>O<sub>5</sub> submicron rods varied with the oxygen concentration, and the responses increased as the oxygen concentration increased at 200°C.

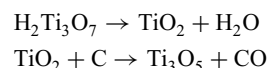
**1. Introduction:** Various properties of 3d transition metal oxides arise from their crystal structures which are generally formed by the linkage of rigid units such as MO<sub>6</sub> octahedra or MO<sub>4</sub> tetrahedra, where M is 3d transition metal ion. As a typical member of 3d transition metal oxides, titanium can exist in a number of suboxide forms (e.g. Ti<sub>2</sub>O<sub>3</sub>, Ti<sub>3</sub>O<sub>5</sub>, Ti<sub>4</sub>O<sub>7</sub>, Ti<sub>5</sub>O<sub>9</sub>) which have important applications in wide range fields, such as catalysts [1], electroconductive ceramics [2], biocompatible coatings [3] and electrochemical components [4]. In recent years, several methods have been developed to obtain suboxide of titanium such as TiO<sub>2</sub> reduction, chemical vapour deposition, and spark plasma sintering. The reduction method is to reduce TiO<sub>2</sub> using different reducing agent, including carbon or H<sub>2</sub> [5], PVA [6], NH<sub>3</sub> [7] and Ti [8]. The chemical vapour deposition [9] can form the materials mainly containing Ti<sub>3</sub>O<sub>5</sub> and Ti<sub>4</sub>O<sub>7</sub>. Ti<sub>1+y</sub>O<sub>2-x</sub> can be fabricated by sintering the mixture of Ti and TiO<sub>2</sub> powder by spark plasma sintering [10]. Compared with other methods, reduction method has distinct advantages in production and technology, and it is applied to prepare substoichiometric titanium oxides.

As a remarkable member of the substoichiometric titanium oxides, Ti<sub>3</sub>O<sub>5</sub> has a variety of structural polymorphisms, including α-Ti<sub>3</sub>O<sub>5</sub>, β-Ti<sub>3</sub>O<sub>5</sub>, γ-Ti<sub>3</sub>O<sub>5</sub>, δ-Ti<sub>3</sub>O<sub>5</sub> and λ-Ti<sub>3</sub>O<sub>5</sub>. It was found that Ti<sub>3</sub>O<sub>5</sub> with different lattice constants have some different interesting properties. Significantly, α-Ti<sub>3</sub>O<sub>5</sub> have small resistance temperature coefficient, strong physical and chemical interaction with adsorbed gas species, as well as β-Ti<sub>3</sub>O<sub>5</sub> [11]. A phase transition between λ-Ti<sub>3</sub>O<sub>5</sub> and α-Ti<sub>3</sub>O<sub>5</sub> occurred at around 450 K with a sharp change in magnetic susceptibility [12]. λ-Ti<sub>3</sub>O<sub>5</sub> can transit to phase β-Ti<sub>3</sub>O<sub>5</sub> with a good optical storage performance, when it is irradiated with ns-pulsed laser light of 532 nm at room temperature [13]. Ti<sub>3</sub>O<sub>5</sub> powder and film can be obtained by hydrogen reduction which is dangerous and requires specialised gas furnaces. In this work, a safety and facile route was described to prepare Ti<sub>3</sub>O<sub>5</sub> submicron rods by sintering H<sub>2</sub>Ti<sub>3</sub>O<sub>7</sub> nanofibres blended with nano-sized carbon black. We have interest to investigate the temperature influence to the reduced phase and the oxygen sensitivity properties of the one dimensional Ti<sub>3</sub>O<sub>5</sub>.

## 2. Experimental details

**2.1. Syntheses:** A 2.0 g portion of anatase TiO<sub>2</sub> nanoparticles and 0.12 g nano-sized carbon black were dispersed in 10M NaOH

solution and the suspension was then transferred into an autoclavable reaction chamber. After that, the reaction chamber was autoclaved in an oven at 180°C for 50 h. The product was filtered after cooling down to room temperature and thoroughly washed with 0.1 M HCl and water to remove any trace of NaCl produced during washing. Subsequently, the material was dried at room temperature. In order to study the phase formation during the reduction process, especially the temperature influence, the as-prepared H<sub>2</sub>Ti<sub>3</sub>O<sub>7</sub> nanofibres blended with nano-sized carbon black were reduced at 1150°C to 1250°C for 3 h. The chemical process can be described as follows



The morphologies and phases structures of the samples were characterised by X-ray diffraction (XRD) and scanning electron microscopy (SEM). The specific surface area of Ti<sub>3</sub>O<sub>5</sub> submicron rods was characterised by Brunauer–Emmett–Teller (BET) method. The conductivity of Ti<sub>3</sub>O<sub>5</sub> submicron rods was tested by four point probes testing system.

**2.2. Sensor fabrication and measurements:** For gas sensing measurement, the as prepared Ti<sub>3</sub>O<sub>5</sub> submicron rods were first mixed with deionised water and then milled to form homogeneous paste. Second, the paste was coated onto the outside surface of a prefabricated ceramic tube to form a smooth film as a sensor. The ceramic tube (with length of 4 mm and diameter of 1 mm) was attached with a pair of gold electrodes and platinum wires. A Ni–Cr heating wire was inserted in the ceramic tube as a heater to control the working temperature by adjusting the heating voltage for the sensor device. In order to stabilise the mechanical properties, the sensor was aged at 100°C for 60 h, meanwhile removing the water and increasing adhesion of Ti<sub>3</sub>O<sub>5</sub> submicro rods with the underlying electrodes. The gas sensing measurement was tented by rejecting or releasing the oxygen gas from the chamber. The concentration of oxygen in the chamber was changed and it was related to the gas sensitivity. The schematic diagram of gas sensing test was shown in Fig. 1,  $V_c$  (mv) is the test circuit voltage,  $V_h$  (mv) is the heating voltage and  $V_{out}$  is the output voltage across the load resistance.

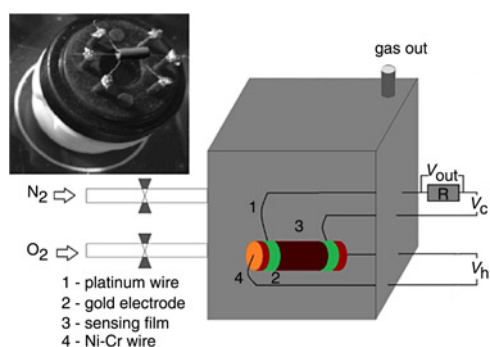


Fig. 1 Schematic of the gas sensing setup

### 3. Discussions

**3.1. Scanning electron microscopy:** The unordered  $\text{H}_2\text{Ti}_3\text{O}_7$  nanofibres with length of 0.4–4  $\mu\text{m}$  blended with nano-sized carbon black can be prepared by hydrothermal method. The carbon black relatively uniformly dispersed in the nanofibres as shown in Fig. 2a. The nanofibres were shorter than those obtained without carbon black because the carbon black partly obstructed the growth of nanofibres. After being reduced at 1250°C for 3 h, the  $\text{H}_2\text{Ti}_3\text{O}_7$  nanofibres changed into  $\text{Ti}_3\text{O}_5$  submicron rods with length of 0.5–2  $\mu\text{m}$  and diameter of 100–300 nm as shown in Fig. 2b. During the synthesis process, some of the packed nanofibres formed rods with larger diameter. Meanwhile, the long nanofibres were broken into short rods as a result of the gas escaping during the reduction reaction.

The specific surface area of the  $\text{Ti}_3\text{O}_5$  submicron rods is 7.806  $\text{m}^2\text{g}^{-1}$  characterised by BET. The  $\text{Ti}_3\text{O}_5$  submicron rods were compacted in a uniaxial press under 20  $\text{kgf}\cdot\text{cm}^{-2}$  pressure into round pellets for measuring its conductivity, and the result showed that the conductivity is 7.828S/cm.

**3.2. X-ray diffraction:** According to the results of the previous study,  $\text{H}_2\text{Ti}_3\text{O}_7$  were transformed into  $\text{TiO}_2$  at 650°C [14], and  $\text{TiO}_2$  can be reduced to  $\text{Ti}_4\text{O}_7$  by carbon at 1100°C in vacuum [15]. In this work, the temperature influence of phase formation during the reduction process has been studied from 1150°C to 1250°C, as shown in Fig. 3. It can be seen that the phase of  $\lambda\text{-Ti}_3\text{O}_5$  appeared at 1150°C, which indicated that  $\text{Ti}_4\text{O}_7$  was further reduced, and the temperature was much higher than theoretical reaction temperature calculated by Gibbs free energy. The further reduction was reacted along with a rise of temperature. At a higher temperature (1175°C), a small amount diffraction peaks of  $\beta\text{-Ti}_3\text{O}_5$  appeared, while the peak intensity of  $\lambda\text{-Ti}_3\text{O}_5$  increased, which indicated further reduction was in progress. When the temperature reached up to 1200°C, the mother phase transformed to  $\lambda\text{-Ti}_3\text{O}_5$ , and the weak diffraction peaks corresponding to  $\text{Ti}_4\text{O}_7$  can be detected. Finally, the phases found in the sample reduced at 1250°C mainly contained  $\lambda\text{-Ti}_3\text{O}_5$  and  $\beta\text{-Ti}_3\text{O}_5$ , and the diffraction peaks of  $\text{Ti}_8\text{O}_{15}$  almost

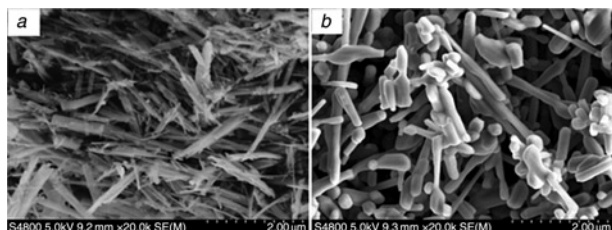


Fig. 2 FE-SEM images of  
a  $\text{H}_2\text{Ti}_3\text{O}_7$  nanofibres  
b  $\text{Ti}_3\text{O}_5$  submicron rods prepared at 1250°C

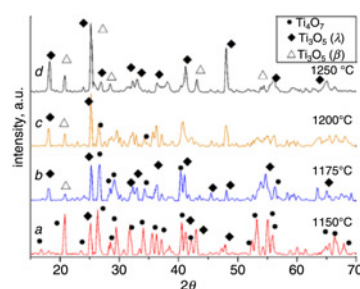


Fig. 3 XRD spectrum of the samples sintered at various temperatures  
a 1150°C  
b 1175°C  
c 1200°C  
d 1250°C

disappeared. The results indicate that the proper reduction temperature for producing  $\text{Ti}_3\text{O}_5$  is 1250°C. It is difficult to synthesis pure form of  $\lambda\text{-Ti}_3\text{O}_5$  or  $\beta\text{-Ti}_3\text{O}_5$  submicron rods due to their similar lattice parameters, and this point is studied in progress. In this study, the oxygen sensing properties of  $\text{Ti}_3\text{O}_5$  submicron rods contained  $\lambda$  and  $\beta$  phase were investigated preliminarily.

**3.3. Oxygen sensing properties:** The sensor based on the as-synthesised  $\text{Ti}_3\text{O}_5$  submicron rods samples was fabricated as mentioned in the experimental section, and the oxygen sensing properties were studied. As known, the operating temperature, atmosphere, gas concentration and other factors can influence the gas sensitivity [16]. In our case, the operating temperature is

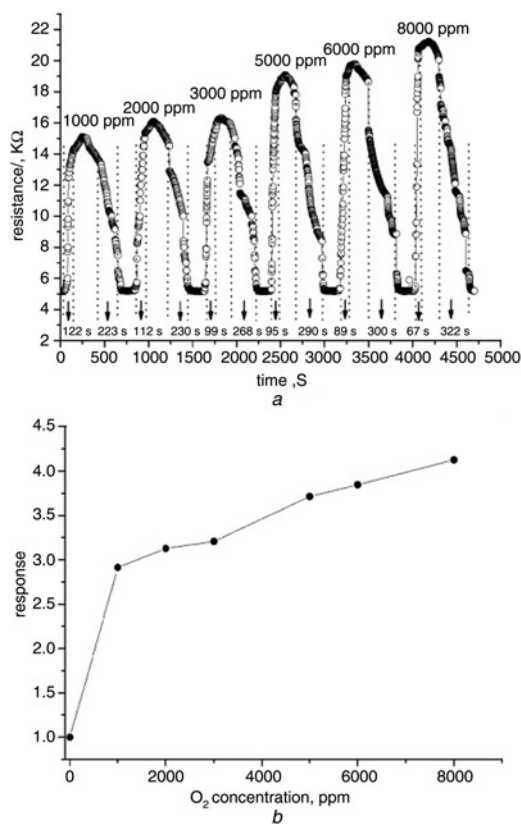


Fig. 4 Oxygen properties of  $\text{Ti}_3\text{O}_5$  submicron rods sensor to different concentrations of oxygen at 200°C  
a Response–recovery curves  
b Response vs concentration curves of  $\text{Ti}_3\text{O}_5$  submicron rods sensor toward oxygen at 200°C

fixed at 200°C and all the test are in oxygen. The oxygen concentration is the key research factor. During the test, the chamber was first filled with nitrogen as background gas, and then a given amount of oxygen was injected. As shown in Fig. 4a, once the sensor contacted with O<sub>2</sub> at 200°C, the resistance increased immediately and gradually reached the maximum value, and subsequently reduced to the initial value when the sensor was transferred into N<sub>2</sub>. The response and recovery time are important factors to assess the gas-sensing properties. Fig. 4a shows that the response and recovery time are long, which demonstrates weak response/recovery capability. In addition, the responses of the sensor increased as the oxygen concentration increased from 1000 to 8000 ppm, as shown in Fig. 4b. The response values are estimated to be 2.91, 3.13, 3.21, 3.71, 3.84, 4.12 at 1000, 2000, 3000, 5000, 6000, 8000 ppm, respectively. The response need to improve for practical application. We will improve the oxygen-sensing properties of Ti<sub>3</sub>O<sub>5</sub> submicron rods by doping with extrinsic dopants or surface treatments in the near future.

Several theoretical models have been built and can be used to explain the gas sensing mechanism [17, 18]. When Ti<sub>3</sub>O<sub>5</sub> was exposed to O<sub>2</sub>, O<sub>2</sub> molecules were adsorbed on its surface by physical absorption, and then the oxygen molecules absorbed in the Ti<sub>3</sub>O<sub>5</sub> surface were transformed into oxygen ions, such as O<sub>2</sub><sup>-</sup>, O<sub>2</sub><sup>2-</sup> and O<sup>-</sup> by chemisorptions. Therefore, the electrons in the conduction band of Ti<sub>3</sub>O<sub>5</sub> would be captured, which reduced the charge carrier concentration and increased the electrical resistance of Ti<sub>3</sub>O<sub>5</sub>. In addition, Ti<sub>3</sub>O<sub>5</sub> belongs to non-stoichiometric oxides and has some oxygen vacancies. It can form lattice oxygen by fusing with oxygen ions. Then the lattice oxygen can form a chemical bond with titanium ions. Hence the balanced oxygen octahedron around these titanium ions could be deformed, leading to structural change between the oxygen and titanium ions in the surface, and a new phase with lower conductivity formed. From the perspective, the oxygen sensing property of Ti<sub>3</sub>O<sub>5</sub> related to the model combining the above two mechanisms can be explained more clearly. Further research and corroboration are needed to study the mechanism of oxygen-sensing property of Ti<sub>3</sub>O<sub>5</sub>.

**4. Conclusions:** In summary, the Ti<sub>3</sub>O<sub>5</sub> submicron rods with larger surface area have been facily synthesised by hydrothermal method combined with carbothermal reduction method. The reaction process and the influence of heating temperature on the synthesis of Ti<sub>3</sub>O<sub>5</sub> submicron rods were discussed. The results indicate that TiO<sub>2</sub> transform to Ti<sub>3</sub>O<sub>5</sub> sintering at 1250°C for 3 h. Sensors based on Ti<sub>3</sub>O<sub>5</sub> submicron rods are fabricated and the oxygen sensing properties mainly investigated. The electric conductivity of the Ti<sub>3</sub>O<sub>5</sub> submicron rods varied with the oxygen concentration at 200°C, which makes it to be potentially used in the field of gas detection.

**5. Acknowledgments:** This work was financially supported by The Open Fund Project from the Key Laboratory of Oil and Gas Material (X151516KCL46, 2016).

## 6 References

- [1] Motojima S., Asakura S., Kasemura T., *ET AL.*: 'Catalytic effect of metal carbides, oxides and Ni single crystal on the vapor growth of the micro-coiled carbon fibers', *Carbon*, 1996, **34**, pp. 289–296
- [2] He L., Franzen H.F., Vitt J.E., *ET AL.*: 'Synthesis and characterization of Ru-Ti<sub>4</sub>O<sub>7</sub> microelectrode arrays', *J. Electrochem. Soc.*, 1994, **141**, pp. 1014–1020
- [3] Botha S.J.: 'Surface properties and bio - acceptability of Ti<sub>2</sub>O<sub>3</sub> surfaces', *Mater. Sci. Eng. A*, 1998, **243**, pp. 221–230
- [4] Smith J.R., Walsh F.C., Clarke R.L.: 'Electrode based on Magneli phase titanium oxides: the properties and application of Ebonex materials', *J. Appl. Electrochem.*, 1998, **28**, pp. 1021–1033
- [5] Dewan M.A.R., Zhang G.Q., Ostrovski O.: 'Carbonothermal reduction of tiania in different gas atmospheres', *Metall. Mater. Trans. B*, 2009, **40**, pp. 62–69
- [6] Toyoda M., Yano T., Tryba B., *ET AL.*: 'Preparation of carbon-coated magneli phases Ti<sub>n</sub>O<sub>2n-1</sub> and their photocatalytic activity under visible light', *Appl. Catal. B: Environ.*, 2009, **88**, pp. 160–164
- [7] Tang C., Zhou D.B., Zhang Q.: 'Synthesis and characterization of magneli phases: reduction of TiO<sub>2</sub> in a decomposed NH<sub>3</sub> atmosphere', *Mater. Lett.*, 2012, **79**, pp. 42–44
- [8] Lu Y., Matsuda Y., Sagara K., *ET AL.*: 'Fabrication and thermoelectric properties of magneli phases by adding Ti to TiO<sub>2</sub>', *Adv. Mater. Res.*, 2012, **1291**, pp. 415–417
- [9] Fredriksson E., Carlsson J.: 'Chemical vapor deposition of titanium oxides in the composition range TiO<sub>1.60</sub>-TiO<sub>1.75</sub>', *Thin Solid Films*, 1985, **124**, pp. 109–116
- [10] Gusev A.A., Avvakumov E.G., Vinokurova O.B.: 'Synthesis of Ti<sub>4</sub>O<sub>7</sub> magneli phase using mechanical activation', *Sci. Sintering*, 2003, **35**, pp. 141–145
- [11] Zheng L.Y., Li G.R., Xu T.X., *ET AL.*: 'Preparation and oxygen sensing properties of α-Ti<sub>3</sub>O<sub>5</sub> thin films', *J. Inorg. Mater.*, 2002, **17**, pp. 1253–1257
- [12] Rao C.N.R., Ramdas S., Loehman R.E., *ET AL.*: 'Semiconductor-metal transition in Ti<sub>3</sub>O<sub>5</sub>', *J. Solid State Chem.*, 1971, **3**, pp. 83–88
- [13] Liu G., Huang W.X., Yi Y.: 'Preparation and optical storage properties of λ-Ti<sub>3</sub>O<sub>5</sub> power', *J. Inorg. Mater.*, 2013, **4**, pp. 425–430
- [14] Han W.Q., Zhang Y.: 'Mageneli phases Ti<sub>n</sub>O<sub>2n-1</sub> nanowires: formation, optical, and transport properties', *Appl. Phys. Lett.*, 2008, **92**, pp. 203117.1–203117.3
- [15] Zhu R.J., Liu Y., Ye J.W., *ET AL.*: 'Magneli phase Ti<sub>4</sub>O<sub>7</sub> powder from carbon thermal reduction method: formation, conductivity and optical properties', *J. Mater. Sci.: Mater. Electron.*, 2013, **24**, pp. 4853–4856
- [16] Wang Y., Kong F.H., Zhu B.L., *ET AL.*: 'Synthesis and characterization of Pd-doped α-Fe<sub>2</sub>O<sub>3</sub> H<sub>2</sub>S sensor with low power consumption', *Mater. Sci. Eng. B*, 2007, **140**, pp. 98–102
- [17] Sun Y.F., Liu S.B., Meng F.L., *ET AL.*: 'Metal oxide nanostructures and their gas sensing properties: a review', *Sensors*, 2012, **12**, pp. 2610–2631
- [18] Zheng L.Y.: 'The preparation and oxygen- sensing properties of α-Ti<sub>3</sub>O<sub>5</sub> thin film', *Sens. Actuators B*, 2003, **88**, pp. 115–119